13th International Conference on
Structural Health Monitoring of Intelligent Infrastructure
DOI: 10.3217/978-3-99161-057-1-123

Prediction of urban wind speed during tropical cyclones using a novel deep learning-based spatiotemporal model

Yuan-Jiang Zeng[1, 2], Zheng-Wei Chen[1, 2], Yi-Qing Ni[1, 2], Pak-Wai Chan[3]
[1]National Rail Transit Electrification and Automation Engineering Technology Research Centre (Hong Kong Branch), Hong Kong, China
[2]Department of Civil and Environmental Engineering, The Hong Kong Polytechnic University, Hong Kong, China
[3]Hong Kong Observatory, Hong Kong, China
email: yuanjiang.zeng@connect.polyu.hk, zhengwei.chen@polyu.edu.hk, ceyqni@polyu.edu.hk, pwchan@hko.gov.hk

ABSTRACT: Tropical cyclones (TCs) stand as one of the most destructive extreme weather events, posing significant threats to human safety and urban infrastructure. One critical phenomenon associated with TCs is the occurrence of strong winds; thus, accurate prediction of urban wind speed during TCs can provide essential information for decision-making, which is vital for enhancing urban resilience. This study proposes a deep learning-based model that accounts for the spatial and temporal dependencies of wind speed data collected from sensors of meteorological stations while addressing the impacts of climate change. The model integrates temporal and spatial encodings with measured time series data, enabling the capturing of long-term temporal dependencies that reflect periodic weather patterns and climate change through the attention mechanism of a Transformer architecture. The outputs derived from this computation are further utilized to identify dynamic patterns of wind speed during TCs. Additionally, a graph neural network (GNN) is integrated to capture spatial dependencies, considering the non-Euclidean distribution of meteorological stations. To evaluate the performance of the proposed model, wind speed measurements from Hong Kong between 2000 and 2023 are used for training and testing. Comparative analyses with sequence-to-sequence models and GNN-recurrent neural network or GNN-Transformer hybrid models demonstrate that the proposed model enhances prediction performance.

KEY WORDS: Tropical cyclones; Wind speed; Transformer; Graph neural network.

1 INTRODUCTION

Urban wind speed is a critical factor influencing human comfort, safety, and urban resilience [1] [2]. Its dynamics directly affect energy management systems [3], infrastructure durability, and ecological balance [4], while extreme wind events, such as tropical cyclones (TCs), pose significant threats to life and property. Rapid urbanization and climate change exacerbates these challenges by intensifying urban heat island effects and creating complex wind environments [5][7], further complicating prediction efforts. Accurate forecasting of urban wind speed, particularly during TCs, is thus essential for effective disaster mitigation, early-warning systems, and urban planning [8].

There are three primary methods for analyzing and predicting urban wind speed: physical models, statistical models, and hybrid models [9]. Physical models rely on geographic information and meteorological fields to solve complex physical equations. For instance, the Weather Research and Forecasting (WRF) model is often combined with complex urban canopy models to predict urban wind speed profiles during TCs [10] [11]. Additionally, WRF can be integrated with computational fluid dynamics (CFD) to investigate time-series wind speed data [12]-[14]. However, these models are typically time-consuming and computationally intensive, which may introduce time lags, and they are sensitive to parameter settings, particularly during extreme TCs.

In contrast, statistical models utilize historical data to develop statistical regressions for predicting future wind speeds. For example, autoregressive moving average (ARMA) models and generalized autoregressive conditional heteroskedasticity (GARCH) models have been employed to forecast seasonal [15] or hourly [16] wind speed. Moreover, model decomposition methods are often integrated with ARMA to enhance wind speed predictions [17]. While statistical models offer rapid inference, they may sacrifice accuracy, especially when wind speed exhibits strong nonstationary behavior [18]. Hybrid models, which combine physical and statistical approaches, aim to leverage the strengths of both methodologies, though they also inherit the limitations of each model type.

Recent advancements in deep learning have attracted considerable attention across diverse fields, such as medicine, transportation, civil engineering, and aerospace, and the application of deep learning for predicting wind speed has also been explored. One approach treats wind speed prediction as a sequence-to-sequence task, employing recurrent neural networks (RNN)-based or convolutional neural networks (CNN)-based models. For instance, long short-term memory (LSTM), gated recurrent unit (GRU), CNN, and CNN-LSTM architectures have been assessed for their performance in long-term wind speed predictions, with forecast horizons ranging from 6 months to 5 years [19]. In addition to long-term predictions, LSTM models have been utilized to forecast 10-minute wind speeds using data from only two measurement sites [9]. Furthermore, ConvLSTM has been employed to predict 10-minute wind speeds based on weather-related images, considering six measurement sites [3]. Beyond RNN- and CNN-based models, Transformer has emerged as a popular alternative for sequence-to-sequence predictions. Various Transformer-based models have been compared for predicting 10-minute wind speeds at three meteorological stations [20].

Another approach incorporates spatiotemporal correlations, rather than treating the problem purely as a sequence-to-

DOI: 10.3217/978-3-99161-057-1-123

sequence task. A notable example of this is the development of a temporal graph convolutional network (TGCN), which combines graph neural networks (GNN) and GRU to predict hourly wind speeds based on data from six measurement stations [21]. However, it is evident that the studies mentioned primarily focus on a limited number of measurement sites, with temporal resolutions typically set at 10 minutes or longer. The prediction of urban wind speed during TCs remains an area requiring further exploration, particularly regarding the application of Transformer-based models that account for spatiotemporal dependencies.

The contributions of this study are three-fold: Firstly, a dense meteorological station network that covers most urban areas is selected, enabling 1-minute resolution wind speed predictions during TCs—an improvement over existing sparse, low-frequency datasets. Secondly, the study develops a novel Transformer-GNN hybrid model that explicitly captures spatial topology through GNN while leveraging Transformer for temporal dependencies, thus advancing beyond conventional sequence-to-sequence approaches. Lastly, a comparison is conducted against current mainstream models, including pure sequence-to-sequence models, GNN-RNN, and GNN-transformer hybrids, demonstrating superior accuracy in extreme wind scenarios and providing valuable insights into spatiotemporal feature engineering for urban meteorology.

The remainder of this paper is structured as follows: Section 2 details the problem formulation, data source and processing, and model architecture. Section 3 presents experimental results with comparative analysis and ablation study, while Section 4 concludes the main findings of this study.

2 METHODOLOGY

2.1 Problem statement

The prediction of urban wind speed during TCs can be framed as a task where, given a series of wind speed measurements from the past P time steps $X_P \in \mathbb{R}^{P\times C}$, the wind speed for the future F time steps $X_F \in \mathbb{R}^{F\times C}$ can be predicted by,

$$X_F = f(X_P) \tag{1}$$

where C represents the number of meteorological stations, and $f(\cdot)$ denotes the deep learning-based models trained. Additionally, the meteorological station network can be described as a graph structure $G = (V, E, A)$, where V represents the nodes (the stations), E indicates the edges, and A denotes the adjacency matrix. The adjacency matrix is established based on the geographic distances between the stations.

2.2 Data source and processing

Hong Kong is located in the southeast of the Pearl River Estuary in southern China, facing the vast South China Sea to the south. It features a long coastline, with most of its low-lying areas concentrated along the coast. Additionally, Hong Kong has a high urbanization rate and is characterized by high-rise buildings, such as the International Finance Centre [22]. These urban and geographical characteristics make Hong Kong vulnerable to TCs [23]. In this study, urban wind speed data collected by 28 meteorological stations from the Hong Kong Observatory (HKO) is used to train and test model performance. It is important to note that the map and locations of the stations shown in Figure 1 are for illustration purposes only; for official information, please refer to the HKO website. The 28 stations cover the main areas of Hong Kong and have maintained continuous data collection over a long period.

Figure 1. Schematic of distribution of meteorological stations.

The data is recorded at a 1-minute interval. A TC is considered to have an effect on Hong Kong if a TC signal has been issued by the HKO. Consequently, data from the entire lifecycle of each TC is extracted. The extracted data for the years 2000-2019 is used as the training set, for 2020-2021 as the validation set, and for 2022-2023 as the test set, as summarized in Table 1. Linear interpolation is employed to address missing data, while the mean and standard deviation are used for normalization and de-normalization.

Table 1. Summary of three data sets.

Data sets	No. of TCs	No. of samples	Rate
Training set	98	920,258	82%
Validation set	11	88,391	8%
Test set	10	115,210	10%

2.3 Model architecture

The model architecture is shown in Figure 2, and it is similar to the logic referenced in [21] [24]-[26]. However, urban wind speed is significantly influenced by TC intensity, which varies with climate change [27], as well as the distance between the TC location and the city. Therefore, this study incorporates long-term dependency, short-term dependency, and spatial dependency to effectively predict future 3-h urban wind speed during TCs using historical 3-h measurements from the meteorological station network. Specifically, both the input length and output horizon are set to 180.

Patch embedding and positional encoding: To improve computational efficiency, this study employs patch embedding to partition the input. Given the input $X_P \in \mathbb{R}^{P\times N}$, patch length L is used for patch embedding to obtain the patched sequence $X^P \in \mathbb{R}^{L\times N\times C}$, where N is the number of patched blocks. Positional encoding $\mathrm{PE}(\cdot)$ is added to the patched blocks using the commonly employed sinusoidal method in Transformer architectures [28], resulting in,

$$X_{enc} = X^P + \mathrm{PE}(X^P) \tag{2}$$

DOI: 10.3217/978-3-99161-057-1-123

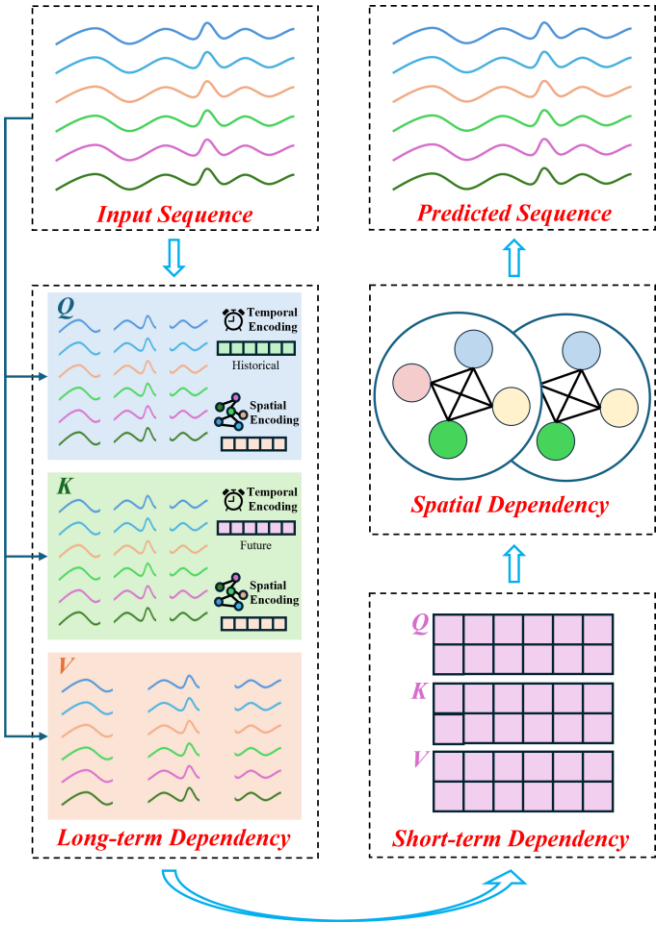

Figure 2. Overview of model architecture.

Temporal encoding and spatial encoding: Climate change [27] and the distance between the TC location and the city significantly influence TC intensity, which in turn affects urban wind speed. However, these factors are not explicitly incorporated into the training process. Regardless of climate change or distance, both are directly related to temporal evolution, which spans from days (for distance) to years (for climate change). Therefore, temporal encoding is necessary to account for both temporal scales.

In this study, temporal encoding is derived by considering various time components: the minute of the hour E^s, the hour of the day E^h, the day of the month E^d, the month of the year E^m, and the year E^y. This encoding embeds more time-related information using linear layers. The components of the temporal encoding are concatenated as follows,

$$E^T = \text{concat}[E^s, E^h, E^d, E^m, E^y] \tag{3}$$

where each E^s, E^h, E^d, E^m, and E^y has a shape of $L \times d/5$ (with d being the embedding dimension), resulting in a final temporal embedding E^T with shape $L \times d$.

Given that meteorological stations are located in various regions with different latitudes, longitudes, and altitudes, it is important to consider the spatial characteristics that may influence urban wind speed. In this study, spatial encoding is employed. Specifically, the normalized Laplacian matrix is calculated as,

$$\Delta = I - D^{-1/2} A D^{-1/2} \tag{4}$$

where I and D are the identity and degree matrices, respectively, and the adjacency matrix is calculated using the latitude, longitude, and altitude of each station. Following this, eigenvalue decomposition is performed as,

$$\Delta = U^T \Lambda U \tag{5}$$

where U and Λ are the eigenvector and eigenvalue matrices. The k smallest non-trivial eigenvectors are then used to generate the spatial encoding $E^S \in \mathbb{R}^{C \times d}$ through linear transformation.

Long-term dependency: Based on the temporal and spatial encodings, temporal dependencies can be more effectively captured by the attention mechanisms of the Transformer architecture. It is important to note that the terms "long-term" and "short-term" differ from those used in the weather prediction field; they are merely used to distinguish between the different horizons considered in this study.

In addition to the long-term effects of climate change on urban wind speed, wind speed exhibits different characteristics across seasons, demonstrating periodic behavior [29]. Thus, long-term dependencies can be implicitly considered, as temporal information is encoded from minutely to yearly. Specifically, long-term dependency is addressed according to the temporal encoding as follows,

$$Q_l^h = w_{ql}^h (E_{his}^T + E^S) \tag{6}$$

$$K_l^h = w_{kl}^h (E_{fut}^T + E^S) \tag{7}$$

$$V_l^h = w_{vl}^h X_{enc} \tag{8}$$

where E_{his}^T is the temporal encoding derived from known historical temporal information, while E_{fut}^T is the temporal encoding derived from future temporal information. The attention mechanism, along with aggregation using the computed attention matrix, can be used to capture the long-term dependency as follows,

$$X_l^h = \text{softmax}\left(\frac{Q_l^h {K_l^h}^T}{\sqrt{d_h}}\right) V_l^h \tag{9}$$

where w_{ql}^h, w_{kl}^h, and w_v^h are learnable parameters for heads h, and d_h is the scaling factor.

Short-term dependency: In addition to long-term dependency, urban wind speed during TCs may vary significantly within a short period as the TCs approach and make landfall in the city. Therefore, short-term dependency is also considered to capture these dynamics. The short-term dependency is addressed by the Transformer architecture based on the known sequence, enabling X_l^h to be used to derive the query, key, and value through commonly used linear layers as follows,

$$Q_s^h = w_{qs}^h X_l^h \tag{10}$$

$$K_s^h = w_{ks}^h X_l^h \tag{11}$$

$$V_s^h = w_{vs}^h X_l^h \tag{12}$$

where w_{qs}^h, w_{ks}^h, and w_{vs}^h are learnable parameters. The short-term dependency can be computed as follows,

DOI: 10.3217/978-3-99161-057-1-123

$$X_s^h = \text{softmax}\left(\frac{Q_s^h K_s^{h^T}}{\sqrt{d_h}}\right) V_s^h \quad (13)$$

Spatial dependency: Spatial dependency is addressed using a graph convolutional neural network (GCN) as follows,

$$G = \delta\left[\alpha X_s + (1-\alpha)\left(w_g \bar{A} X_s\right)\right] \quad (14)$$

where w_g are the learnable parameters and $\bar{A}$ is the normalized adjacency matrix. After aggregating spatial information, α balances the previous information with the aggregated information, and δ is a function used to reduce overfitting.

Residual connections are then utilized as follows,

$$O^{(l)} = \text{SwiGLU}\left[\text{RMSN}\left(G^{(l)} + O^{(l-1)}\right)\right] + G^{(l)} \quad (15)$$

where $O^{(l)}$ and $O^{(l-1)}$ represent the outputs of layer l and layer l-1 of the aforementioned spatiotemporal dependency computation layer, respectively. Here, SwiGLU denotes the activation function, and RMSN represents the RMSNorm [30].

2.4 Experimental setup

In this study, three types of models are selected to compare their performance with the proposed model, representing three typical categories: statistical model, pure sequence-to-sequence models, and hybrid models combining GNN-RNN or GNN-Transformer architectures. The ARMA model is chosen as the baseline for statistical models, while LSTM, GRU, and vanilla Transformer models are selected as pure sequence-to-sequence models. For hybrid models, TGCN [26] is chosen for the GNN-RNN approach, and PDFormer [25] is selected for the GNN-Transformer approach.

The model setup for ARMA is derived from [16], where sensitivity analysis is performed. The configurations for TGCN and PDFormer follow the original papers [25] [26]. For GRU and LSTM, the number of RNN layers and embedding dimensions match those of TGCN [26], while the number of blocks and embedding dimensions for the Transformer align with the proposed model in this study. The specific configurations include an embedded dimension of 250, a Laplacian dimension for generating spatial encoding of 8, five heads for computing temporal dependency, a depth of 3 for spatiotemporal dependency computation, a drop rate of 0.1 for attention computation, and a linear drop rate within the range of [0, 0.1] for each depth.

2.5 Evaluation metrics

To evaluate the model's performance, three metrics are used: mean absolute error (MAE), root mean square error (RMSE), and the R^2 score.

$$\text{MAE} = \frac{1}{n}\sum|y - \hat{y}| \quad (16)$$

$$\text{RMSE} = \sqrt{\frac{1}{n}\sum(y - \hat{y})^2} \quad (17)$$

$$\text{R}^2 = 1 - \frac{\sum(y-\hat{y})^2}{\sum(y-\bar{y})^2} \quad (18)$$

where y, $\hat{y}$, and $\bar{y}$ represent the target values, predicted values, and mean value of urban wind speed, respectively, while n denotes the total number of urban wind speed values. A lower MAE and RMSE signify superior model performance. Additionally, a higher R^2 score reflects improved model performance.

2.6 Optimization details

For each model, training is conducted three times, with the best result selected for performance evaluation. Each training session is set for a large number of epochs, and an early stopping mechanism is implemented to avoid overfitting. The batch size is set to 256, the learning rate is 0.0003, and *Adam* is employed as the optimizer. Mean squared error is chosen as the loss function. The programming is carried out using Python and PyTorch, with models trained on an RTX-6000 Ada GPU card featuring 48GB VRAM and 512GiB of system memory.

3 RESULTS AND DISCUSSIONS

3.1 Evaluation of model's performance

The model's performance is summarized in Table 2. It is evident that the conventional statistical model struggles to deliver reliable predictions in scenarios involving extreme wind speeds across the entire network of stations. The MAE of the ARMA model is approximately three times greater than that of the other deep learning models listed in Table 2, while the RMSE for ARMA is five times larger than that of the other models. Additionally, the R^2 score indicates that the predicted results exhibit greater fluctuations compared to those generated by the deep learning models.

Table 2. Summary of model's performance.

Models	MAE	RMSE	R^2
ARMA	3.230	7.600	0.6539
LSTM	1.103	1.593	0.8638
GRU	0.990	1.464	0.8849
Transformer	0.909	1.376	0.8985
TGCN	0.919	1.372	0.8989
PDFormer	0.914	1.360	0.9007
Proposed	0.902	1.348	0.9026

Regarding the sequence-to-sequence models, the results indicate that the Transformer outperforms the other two models (GRU and LSTM) across all metrics, including MAE, RMSE, and R^2 score. This demonstrates the Transformer's superior ability to capture temporal dependencies. However, compared to the GNN-RNN and GNN-Transformer hybrid models, the pure sequence-to-sequence models tend to yield less reliable predictions. This suggests that spatial dependencies are not adequately addressed in these models, leading to decreased performance. Notably, both LSTM and GRU exhibit larger errors compared to TGCN and PDFormer. While the Transformer has a smaller MAE, it also shows a larger RMSE and a lower R^2 score compared to the two hybrid models. This indicates that, despite the Transformer's average performance being slightly better than that of TGCN and PDFormer, it may be less effective in predicting extreme values.

Regarding the hybrid models, the proposed model demonstrates superior performance in predicting urban wind speed across all metrics. It exhibits smaller errors compared to the other two hybrid models that also incorporate spatial dependency computation, as well as the pure sequence-to-sequence models. Notably, while TGCN and PDFormer have larger MAE values than the Transformer, the proposed model achieves smaller error rates than all other models listed in Table

DOI: 10.3217/978-3-99161-057-1-123

2. This highlights the effectiveness of the proposed model in addressing both temporal and spatial dependencies in urban wind speed prediction.

3.2 Ablation study

To illustrate the role of the modules in the proposed model, an ablation study is conducted. The first experiment (Delete-LTD) involved removing the long-term dependency module, the second experiment (Delete-STD) removed the short-term dependency module, and the third experiment (Delete-SD) eliminated the spatial dependency module. In these three additional experiments, all other components (except for the deleted modules) are maintained exactly as in the proposed model (Full). The MAE, RMSE, and R^2 scores from these experiments are presented in Figure 3.

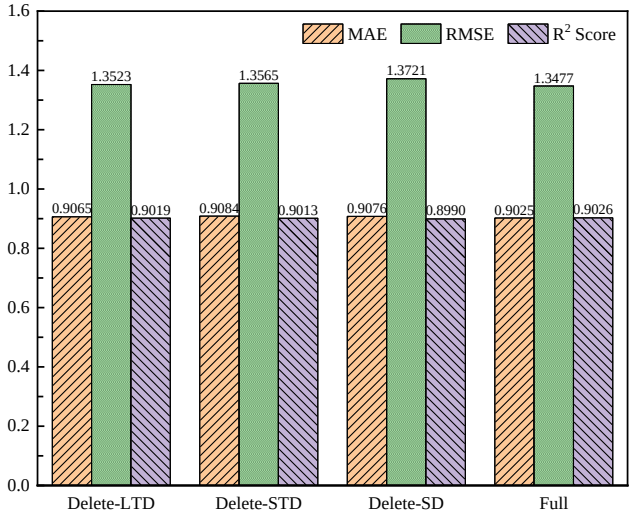

Figure 3. Performance comparison of ablation study experiments.

The results indicate that removing any component from the proposed model leads to a decrease in performance based on the evaluation metrics. This finding clarifies the contributions of each module to the overall effectiveness of the model, underscoring the significance of long-term, short-term, and spatial dependencies in achieving accurate predictions. Each module plays a crucial role in enhancing the model's ability to capture the complexities of urban wind speed dynamics.

When the GNN module is removed, the model resembles the vanilla Transformer, resulting in the outcome of experiment Delete-SD being closer to that of the vanilla Transformer listed in Table 2. However, the result of experiment Delete-SD is slightly better than the vanilla Transformer. This can be explained by the fact that the vanilla Transformer primarily focuses on correlations within the known sequence (the short-term dependencies in this study). When both short-term and long-term dependencies are incorporated, the performance improves slightly. On the other hand, the experiment Delete-SD does not perform as well as the proposed model due to the absence of the GNN module. This highlights the importance of the GNN in enhancing the performance of urban wind speed prediction. The presence of the GNN significantly contributes to capturing the spatial dependencies, resulting in more accurate predictions.

In the experiments Delete-LTD and Delete-STD, the results are similar, but neither provides better predictions than the proposed model. This indicates that both long-term and short-term dependencies are crucial for achieving accurate predictions. Furthermore, the results of these two experiments are better than those of the Delete-SD experiment, which further underscores the importance of spatial dependency in enhancing model performance. This highlights the necessity of integrating all three types of dependencies for optimal prediction accuracy in urban wind speed prediction.

3.3 Case study

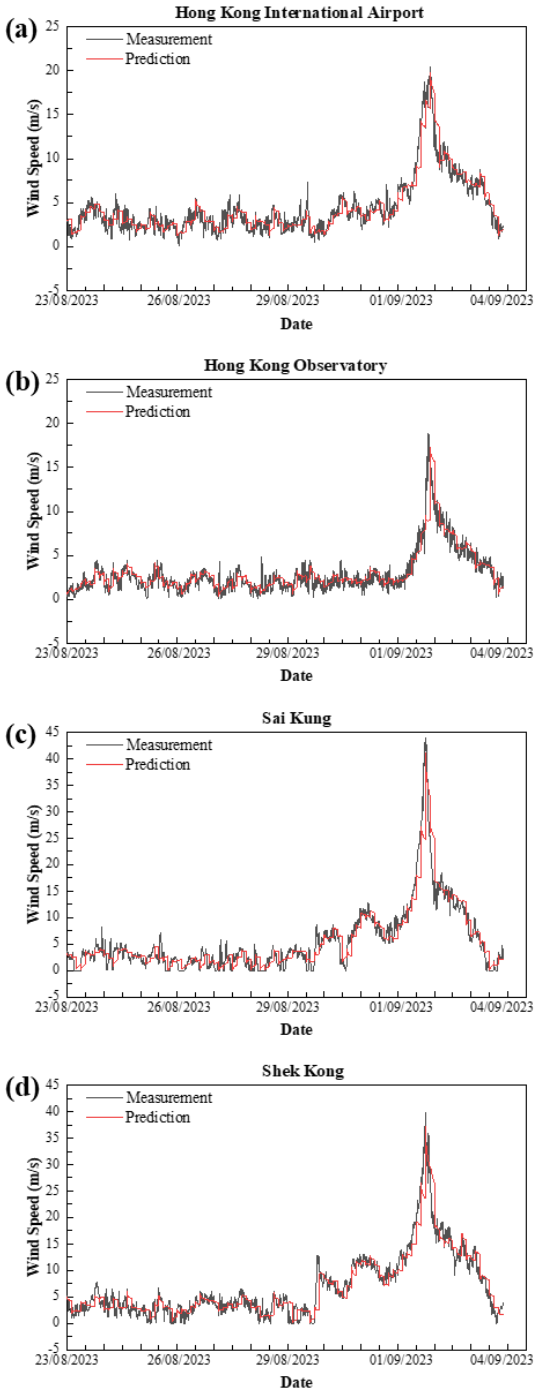

Figure 4. Wind speed prediction of four stations during Typhoon Saola.

DOI: 10.3217/978-3-99161-057-1-123

To illustrate predicted urban wind speeds, two case studies are conducted: Typhoon Saola and Typhoon Koinu. Saola, the third TC in Hong Kong in 2023, prompted signal No. 10, the first since Super Typhoon Mangkhut in 2018. Koinu triggered signal No. 9 and brought heavy rain, with 369.7 millimeters recorded—over three times the normal monthly total and the highest daily rainfall for October.

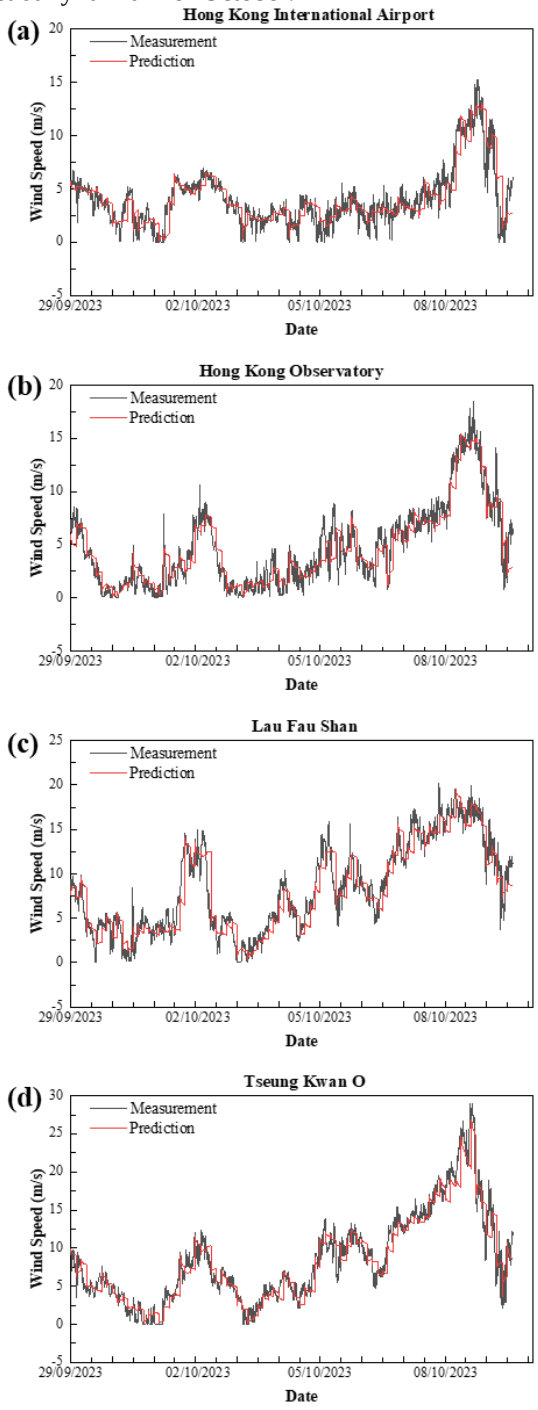

Figure 5. Wind speed prediction of four stations during Typhoon Koinu.

For Typhoon Saola, four stations—Hong Kong International Airport (HKA), HKO, Sai Kung, and Shek Kong—are selected to illustrate the predicted wind speed, as shown in Figure 4. The selection of these stations is based on two key principles: first, HKA and HKO were chosen for their strategic locations; second, the remaining stations were selected due to their relatively higher measured wind speed during the cyclone, with an emphasis on decentralization. Similarly, for Typhoon Koinu, HKA, HKO, Lau Fau Shan, and Tseung Kwan O were selected to represent the predicted wind speed, as depicted in Figure 5.

The proposed model demonstrates strong predictive capabilities for the two selected cases. The trends in the predictions align closely with the target measurements, even as wind speeds increase when the TCs approach Hong Kong. However, it is evident that the model tends to underestimate the peak values, which may be attributed to the inherent tendency of neural networks to produce smoother outputs—a phenomenon commonly observed in many deep learning models. Additionally, the results for Typhoon Saola are more consistent with the measurements than those for Typhoon Koinu. This discrepancy may be partially due to the fewer local peaks observed during Typhoon Saola, as well as the model's limitations in effectively capturing peak wind speeds.

4 CONCLUSIONS

In this study, a novel deep learning-based spatiotemporal model is proposed for predicting urban wind speed during TCs. The following key conclusions can be drawn:

- The proposed model achieves better prediction accuracy compared to the statistical model and pure sequence-to-sequence models, with a MAE of 0.902. This represents a 0.78% improvement over the vanilla Transformer, a 9.76% improvement over GRU, and a 22.28% improvement over LSTM. Additionally, it outperforms GNN-RNN and GNN-Transformer hybrid models by more than 1%.
- The vanilla Transformer demonstrates potential in predicting urban wind speed during TCs. The proposed model's integration of long-term, short-term, and spatial dependencies significantly enhances its performance compared to the vanilla Transformer. This improvement underscores the importance of considering various types of dependencies in achieving more accurate predictions in complex environments like urban areas during TCs.
- The proposed model effectively captures the trends in urban wind speed during TCs. Specific case studies reveal strong performance in predicting peak values for Typhoon Saola; however, some smoother predictions were observed for Typhoon Koinu.

ACKNOWLEDGMENTS

This work was supported by the Research Grants Council of the Hong Kong Special Administrative Region, China (Grant No. T22-501/23-R), and the Innovation and Technology Commission of the Hong Kong Special Administrative Region, China (Grant No. K-BBY1). The authors would like to express their gratitude for the computing platform provided by the University Research Facility in Big Data Analytics (UBDA) at The Hong Kong Polytechnic University, as well as for the data supplied by the Hong Kong Observatory, which was used solely for research purposes.

DOI: 10.3217/978-3-99161-057-1-123

REFERENCES

[1] J. Ngarambe, J. W. Oh, M. A. Su, M. Santamouris, G. Y. Yun, Influences of wind speed, sky conditions, land use and land cover characteristics on the magnitude of the urban heat island in Seoul: An exploratory analysis, Sustainable Cities and Society, 71 (2021) 102953.
[2] S. J. Low, V. S. Raghavan, H. Gopalan, J. C. Wong, J. Yeoh, C. C. Ooi, FastFlow: AI for fast urban wind velocity prediction, 2022 IEEE International Conference on Data Mining Workshops (ICDMW), 2022.
[3] L. Zheng, W. Lu, Q. Zhou, Weather image-based short-term dense wind speed forecast with a ConvLSTM-LSTM deep learning model, Building and Environment, 239 (2023) 110446.
[4] G. Liu, X. Wang, Q. Wu, D. Fang, Z. Wu, H. Liu, M. Lyu, Effect of urbanization on gust wind speed in summer over an urban area in Eastern China, Environmental Research Letters, 18 (7) (2023) 074025.
[5] J. W. Wang, H. J. Yang, J. J. Kim, Wind speed estimation in urban areas based on the relationships between background wind speeds and morphological parameters, Journal of Wind Engineering and Industrial Aerodynamics, 205 (2020) 104324.
[6] J. Allegrini, V. Dorer, J. Carmeliet, Influence of morphologies on the microclimate in urban neighbourhoods, Journal of Wind Engineering and Industrial Aerodynamics, 144 (2015) 108-117.
[7] Y. Abbassi, H. Ahmadikia, E. Baniasadi, Impact of wind speed on urban heat and pollution islands, Urban Climate, 44 (2022) 101200.
[8] P. Peduzzi, B. Chatenoux, H. Dao, A. De Bono, C. Herold, J. Kossin, F. Mouton, O. Nordbeck, Global trends in tropical cyclone risk, Nature Climate Change, 2 (4) (2012) 289-294.
[9] Y. Hao, W. Yang, K. Yin, Novel wind speed forecasting model based on a deep learning combined strategy in urban energy systems, Expert Systems with Applications, 219 (2023) 119636.
[10] Y. Zhang, S. Cao, L. Zhao, J. Cao, A case application of WRF-UCM models to the simulation of urban wind speed profiles in a typhoon, Journal of Wind Engineering and Industrial Aerodynamics, 220 (2022) 104874.
[11] F. Salamanca, A. Martilli, M. Tewari, F. Chen, A study of the urban boundary layer using different urban parameterizations and high-resolution urban canopy parameters with WRF, Journal of Applied Meteorology and Climatology, 50 (5) (2011) 1107-1128.
[12] J. Wang, L. Wang, R. You, Evaluating a combined WRF and CityFFD method for calculating urban wind distributions, Building and Environment, 234 (2023) 110205.
[13] R. Kadaverugu, V. Purohit, C. Matli, R. Biniwale, Improving accuracy in simulation of urban wind flows by dynamic downscaling WRF with OpenFOAM, Urban Climate, 38 (2021) 100912.
[14] Y. Miao, S. Liu, B. Chen, B. Zhang, S. Wang, S. Li, Simulating urban flow and dispersion in Beijing by coupling a CFD model with the WRF model, Advances in Atmospheric Sciences, 30 (6) (2013) 1663-1678.
[15] Z. Guo, Y. Dong, J. Wang, H. Lu, The forecasting procedure for long-term wind speed in the Zhangye area, Mathematical Problems in Engineering, 2010 (1) (2010) 684742.
[16] E. Grigonytė, E. Butkevičiūtė, Short-term wind speed forecasting using ARIMA model, Energetika, 62 (1-2) (2016).
[17] H. Liu, H. Tian, Y. Li, An EMD-recursive ARIMA method to predict wind speed for railway strong wind warning system, Journal of Wind Engineering and Industrial Aerodynamics, 141 (2015) 27-38.
[18] Z. Huang, M. Gu, Characterizing nonstationary wind speed using the ARMA-GARCH model, Journal of Structural Engineering, 145 (1) (2019) 04018226.
[19] M. Yaghoubirad, N. Azizi, M. Farajollahi, A. Ahmadi, Deep learning-based multistep ahead wind speed and power generation forecasting using direct method, Energy Conversion and Management, 281 (2023) 116760.
[20] C. Yu, G. Yan, C. Yu, X. Liu, X. Mi, MRIformer: A multi-resolution interactive transformer for wind speed multi-step prediction, Information Sciences, 661 (2024) 120150.
[21] Z. Chen, B. Zhang, C. Du, W. Meng, A. Meng, A novel dynamic spatio-temporal graph convolutional network for wind speed interval prediction, Energy, 294 (2024) 130930.
[22] C. Song, C. Sun, J. Xu, F. Fan, Establishing coordinated development index of urbanization based on multi-source data: A case study of Guangdong-Hong Kong-Macao Greater Bay Area, China, Ecological Indicators, 140 (2022) 109030.
[23] W. Chen, S. Yang, Z. Wu, F. Cai, Large-scale atmospheric features favoring the tropical cyclone activity affecting the Guangdong–Hong Kong–Macao Greater Bay Area of China, Environmental Research Letters, 17 (10) (2022) 104057.
[24] Z. Li, L. Xia, L. Shi, Y. Xu, D. Yin, C. Huang, Opencity: Open spatio-temporal foundation models for traffic prediction, arXiv preprint arXiv:2408.10269, (2024).
[25] J. Jiang, C. Han, W. X. Zhao, J. Wang, PDFormer: Propagation delay-aware dynamic long-range transformer for traffic flow prediction, Proceedings of the AAAI conference on artificial intelligence, 2023.
[26] L. Zhao, Y. Song, C. Zhang, Y. Liu, P. Wang, T. Lin, M. Deng, H. Li, T-GCN: A temporal graph convolutional network for traffic prediction, IEEE Transactions on Intelligent Transportation Systems, 21 (9) (2019) 3848-3858.
[27] I. J. Moon, S. H. Kim, J. C. Chan, Climate change and tropical cyclone trend, Nature, 570 (7759) (2019) E3-E5.
[28] A. Vaswani, N. Shazeer, N. Parmar, J. Uszkoreit, L. Jones, A. N. Gomez, Ł. Kaiser, I. Polosukhin, Attention is all you need, Advances in neural information processing systems, 2017.
[29] I. Deligiannis, P. Dimitriadis, O. Daskalou, Y. Dimakos, D. Koutsoyiannis, Global investigation of double periodicity of hourly wind speed for stochastic simulation; Application in Greece, Energy Procedia, 97 (2016) 278-285.
[30] N. Shazeer, GLU variants improve Transformer, arXiv preprint arXiv:2002.05202, (2020).